ELSEVIER

Chemical Geology 200 (2003) 25–40

CHEMICAL GEOLOGY
INCLUDING
ISOTOPE GEOSCIENCE

www.elsevier.com/locate/chemgeo

Antimony isotope variations in natural systems and implications for their use as geochemical tracers

Olivier Rouxel[a,*], John Ludden[a,1], Yves Fouquet[b,2]

[a] *CRPG-CNRS, 15 rue Notre Dame des Pauvres, 54501 Vandoeuvre les Nancy, France*
[b] *IFREMER DRO/GM, BP 70, 29280 Plouzané, France*

Received 7 October 2002; accepted 23 February 2003

Abstract

Multiple-collector inductively coupled plasma mass spectrometry (MC-ICP-MS) has been used for the precise measurement of Sb isotopic composition in geological samples, as well as Sb(III) and Sb(V) species in aqueous samples. Sb is chemically purified prior to analysis by using cation-exchange resin and cotton impregnated with thioglycollic acid (TCF). Purification through cation-exchange resin is required for the removal of matrix interfering elements such as transitional metals, whereas TCF is required for the separation of other hydride-forming elements such as Ge and As. The analyte is introduced in the plasma torch using a continuous flow hydride generation system. Instrumental mass fractionation is corrected with a ''standard-sample bracketing'' approach. Using this technique, the minimum Sb required per analysis is as low as 10 ng for an estimated external precision calculated for the $^{123}Sb/^{121}Sb$ isotope ratio of 0.4 ε units (2σ).

Sb isotope fractionation experiments reported here indicate strong fractionation (9 ε units) during Sb(V) reduction to Sb(III). Seawater, mantle-derived rocks, various environmental samples, deep-sea sediments and hydrothermal sulfides from deep-sea vents have been analyzed for their Sb isotope composition. We define a continental and oceanic crust reservoir at 2 ± 1 ε units. Seawater $\varepsilon^{123}Sb$ values do not vary significantly with depth and yield a restricted range of 3.7 ± 0.4 ε units. Sb deposited in hydrothermal environments has a significant range of Sb isotopic composition (up to 18 ε units). These variations may reflect not only contributions from different Sb-sources (such as seawater and volcanic rocks), but also kinetic fractionation occurring at low temperature in aqueous media through the reduction of seawater-derived Sb(V) in more reducing environment. Our results suggest that Sb isotopes can be extremely useful tracers of natural processes and may be useful as paleoredox tracers in oceanic systems.

Keywords: Antimony; Stable isotopes; Multicollector ICP-MS; Trace elements; Hydrothermal systems; Basalts

1. Introduction

Over the past 5 years, unprecedented advances have been made for high-precision measurement of isotopic compositions due to the development of multiple-collector magnetic sector inductively coupled plasma mass spectrometry (MC-ICP-MS). This technique

* Corresponding author. Present address: Department of Earth Sciences, University of Cambridge, Downing Street, Cambridge CAMBS CB2 3EQ, UK. Tel.: +44-1223-333405; fax: +44-1223-333450.

E-mail addresses: orou02@esc.cam.ac.uk (O. Rouxel), john.ludden@cnrs-dir.fr (J. Ludden), fouquet@ifremer.fr (Y. Fouquet).

[1] Fax: +33-1-44-96-49-08.

[2] Fax: +33-2-98-22-45-70.

0009-2541/03/$ - see front matter © 2003 Elsevier Science B.V. All rights reserved.
doi:10.1016/S0009-2541(03)00121-9

combines the high ionization efficiency of the Ar plasma source with the magnetic sector/multiple collector, a measuring device providing precise and accurate isotope ratio determination. In particular, the studies of the stable isotope systematics of metals, such as Fe (Belshaw et al., 2000), Cu (Maréchal et al., 1999; Zhu et al., 2000), Zn (Maréchal et al., 2000), Mo (Barling et al., 2001), Tl (Rehkämper and Halliday, 1999) and metalloid Se (Rouxel et al., 2002), are now routinely performed on MC-ICP-MS and provide new insights into planetary processes and cosmochemistry as well as natural fractionation of isotopes in inorganic and biological processes on the earth.

Sb has two stable isotopes of mass 121 and 123 with average abundances of 57.362% and 42.638%, respectively (Anders and Grevesse, 1989). To date, no geochemical or cosmochemical investigations of the variations of these isotopes have been attempted. In fact, the development of Sb isotope measurements for geochemical studies is challenging as Sb isotopes have low mass differences (1.6%) precluding large mass fractionation in nature and Sb is a trace element below 100 ng/g for most geological samples and below 300 ng/l for seawater.

Antimony is undoubtedly an interesting element in many aspects. It is a moderately siderophile element that behaves like the incompatible lithophile element Pr during igneous processes in the mantle (Jochum and Hofmann, 1997) with concentrations varying from 0.02 to 0.8 ppm in oceanic basalts. Furthermore, antimony behaves as a highly incompatible element during the formation of continental crust, but it is only moderately incompatible during the formation of oceanic basalts. This "bimodal incompatibility" may be related to the transfer through the upper continental crust by hydrothermal processes acting in conjunction with normal igneous processes (Noll et al., 1996; Sims et al., 1990).

Chemically similar to arsenic, Sb can be found mainly as inorganic Sb(V) and Sb(III) species but volatile species (SbH_3) and methylated species may occur in natural environments (Andreae et al., 1981). It has been clearly shown that the toxicity of Sb species is similar to that of As, with Sb(III) being much more poisonous than Sb(V) (Gurnani et al., 1994). Therefore, numerous studies have been focused on the measurement (Yu et al., 1983) and distribution of Sb species and their redox transformations in order to understand the environmental consequences of their presence in aquatic systems (Brannon and Patrick, 1985; Thanabalasingam and Pickerign, 1990; Belzile et al., 2001). In oxygenated waters, the antimonate ion $Sb(OH)_6^-$ should be the thermodynamically stable form of Sb (Turner et al., 1981). Although aqueous antimony chloride complexes have been observed, it is generally believed that aqueous antimony sulfide complexes dominate in most conditions (Sherman et al., 2000). A significant fraction of the total Sb measured in natural waters can also be present as Sb(III), methylstibonic acid and dimethylstibine (Andreae et al., 1981). The presence of the nonequilibrium species is probably due to biological activity and kinetic processes (Andreae, 1983). The biogeochemistry of Sb is thus controlled by the chemical speciation of the dissolved forms, which can be altered under different redox conditions.

Kinetic reduction of metals and metalloid compounds, such as Fe (Matthews et al., 2001), Cr (Ellis et al., 2002), Cu (Zhu et al., 2002) and Se (Johnson et al., 1999), is known to produce large isotope fractionation among the formed reduced species and the residual oxidized species. Therefore, it is anticipated that redox changes of Sb(V) and Sb(III) species as well as biological activity and Sb volatilization or transport in hydrothermal systems can produce significant isotope fractionation in natural systems.

In this study, we report on a technique for the isotopic analysis of Sb in geological samples and Sb(III), Sb(V) species in aqueous samples using a continuous-flow hydride generation (HG) system coupled to a Micromass *Isoprobe* multicollector inductively coupled plasma mass spectrometry (MC-ICP-MS). As previously used for Se isotopes (Rouxel et al., 2002), this technique applied to Sb isotopes should meet the requirement of the high-precision isotope analyses using MC-ICP-MS and high sensitivity reached by analysis of gaseous hydride. We present data from experimental investigation of Sb isotope fractionation during reduction of Sb(V) to Sb(III) to provide an assessment of the potential of using Sb isotope as a new geochemical tracer. Preliminary studies of Sb isotope composition in natural environment are also presented for mantle-derived rocks, sediments, hydrothermal sulfides and seawater.

2. Analytical methods

2.1. Reagents

Water was purified using a Millipore deionizing system. Distilled nitric and hydrochloric acids were used for the chemical separation and hydride generation. All glassware and Teflon© (PTFE) materials were cleaned with concentrated analytical reagent grade nitric acid and distilled water before use. Sodium borohydride (MERCK Eurolab) solution at 1% (m/v) was prepared daily after filtration and was stabilized in 0.05% (m/v) NaOH. A reducing solution of KI (10%) was prepared by dissolving KI salt (prolabo analytical grade) in distilled water with 10% ascorbic acid (prolabo analytical grade). A standard Sb solution was obtained from Spex solution and stabilized in 0.001% ascorbic acid.

Thiol cotton fiber (hereafter abbreviated as TCF) used for Sb enrichment is prepared using the following procedure described by Yu et al. (1983) and Marin et al. (2001). Thioglycollic acid (62.6 ml), acetic anhydride (34.7 ml), acetic acid (16.5 ml) and concentrated sulfuric acid (0.137 ml) were put in PTFE beaker and mixed well and 10 g of hydrophile cotton (medical grade) was introduced. The beaker was closed and left for 4 days in a water bath at 40 °C. The beaker was agitated every day. The TCF was filtered using a sintered-glass funnel and washed with water. The TCF was dried at room temperature for 2 days in a clean box.

2.2. Chemical purification of geological samples

Less than 400 mg of sample (silicates and sulfides), corresponding to approximately 50 ng of Sb, was digested in concentrated HF (8 ml), HNO_3 (1 ml) and $HClO_4$ (0.05 ml) in 10 ml PTFE digestion vessel. Before sealing, the PTFE containers with sulfide-rich or carbonate-rich materials were left at room temperature until completely degassed. For the organic-rich material (e.g. soil, shale), 4 ml of concentrated HNO_3 and 1 ml H_2O_2 + 1 ml HF were first added and taken to incipient dryness at 40 °C. Sealed PTFE containers were left overnight on hot plates at 100 °C and were then brought to incipient dryness at 80 °C.

The residue obtained after chemical dissolution was dissolved in 5 ml of 0.12 N HF and the solution was heated in a closed vessel at 80 °C in boiling water bath and ultrasonicated. Solid residues were removed by centrifugation and the solution was then loaded on cation exchange chromatographic columns (Biorad AG50-X8) filled with 2.5 ml of resin (wet volume). The column was regenerated with 10 ml of 6 N HCl and conditioned with 5 ml of H_2O. The solution that passed through the column contains Sb(V) and other anions (such as sulfate, chlorides, and Ge, As, Se) whereas the matrix (including iron) is strongly adsorbed on the resin. A final wash with 4 ml of H_2O elutes residual Sb. For Fe-rich samples or more than 250 mg of sample, the chemical purification (including regeneration of the resin) is repeated to ensure that the matrix is quantitatively removed from the sample. As Sb is only passing through the column under this chemical procedure, complete recovery of Sb is achieved without inducing any isotopic bias.

Sb(V) is reduced to Sb(III) by adding 0.5 ml of a 10% KI solution stabilized in 10% ascorbic acid. The reduction is enhanced by adjusting the solution to 1 N HCl and by allowing 24-h settling time. Quantitative reduction may also be achieved within several minutes as suggested by Petrick and Krivan (1987) by heating the solution, but the temperature must be kept below 90 °C as ascorbic acid tends to decompose at high temperature and high HCl concentration.

After this reduction step, the solution in 1 N HCl was diluted to 0.5 N HCl with H_2O and then loaded on a 10-ml column filled with 0.14 g of TCF previously washed with 5 ml H_2O and conditioned with 5 ml of 0.5 N HCl. Sb was eluted slowly with 2.5 ml of 6 N HCl and then diluted with 2.5 ml of H_2O after adding 0.5 ml KI and ascorbic acid at 10% to prevent back oxidation of Sb(III) for hydride generation analysis. Other hydride-forming elements, Se, As and the isobaric interfering element Te, are retained in the cotton as already observed by Yu et al. (1983). The use of a mixture of KI and ascorbic acid in the chemical preparation further improves the chemical separation of Sb from Te, which has an isobaric interference with ^{123}Sb due to the formation of unreactive Te° species.

2.3. Sb(III) and Sb(V) determination in aqueous sample water

It has been noted (Yu et al., 1983) that within certain pH ranges, the Sb(V) species are partly reduced to Sb(III) by the thiol groups of the cotton and are absorbed. This impairs the selectivity of Sb(III) speciation. Thus, for better selectivity in the presence of Sb(V), Sb(III) is adsorbed on TCF from pH 5 to 8, which is the common pH range for most natural waters including seawater. Sb(III) is then desorbed as for total Sb determination and residual Sb(V) is converted to Sb(III) with a mixture of KI and ascorbic acid at 0.2% in 0.5 N HCl medium and is processed for chemical separation following the procedure for total Sb determination. The same TCF column was used for the determination of the two Sb species in the same sample as no difference was observed with the use of a new TCF column.

2.4. HG-MC-ICP-MS isotope ratio measurement

The generation of Sb hydride (SbH_3) is among the most suitable techniques for on-line separation and speciation of nanogram amounts of Sb. Different oxidation states of Sb exhibit different sensitivity in HG technique, with Sb(III) being more sensitive to Sb(V) species (Dedina and Tsalev, 1995). The hydride generation system used for Sb isotope analysis is similar to the system used for Se isotope determination (Rouxel et al., 2002) and is shown schematically in Fig. 1. Operating parameters of the HG are summarized in Table 1. A peristaltic pump was used to deliver the reducing agent and the sample to the hydride generation system. For the gas–liquid separator, we used a modified Scott-type spray chamber cooled at 4 °C without the nebulizer in place. After the gas–liquid separator and aerosol filter, the Sb hydrides are transported via Teflon tubing directly to the ICP torch. Stability of the hydride formation was improved by the mixing coil (20 cm), consistent pumping of the liquid waste to the drain and a second Ar inlet placed between the gas–liquid separator and the ICP-MS torch. The *Isoprobe*, operating at the Centre de Recherches Pétrographiques et Géochimi-

Table 1
HG-MC-ICP-MS operating conditions

Inductively coupled plasma	
RF power	1450 W
Plasma Ar flow rate	13 l min^{-1}
Intermediate Ar flow rate	1.1 l min^{-1}
Mass spectrometer	
Sample	Nickel
Skimmer	Nickel
Ar hexapole flow rate	1.8 ml min^{-1}
Data acquisition parameters	
Measurement time/sequence	8 s
Number of raw data	25
Z1–Z2: 10 s	
Hydride generation	
Reducing agent	1% (m/v) $NaBH_4$ in 0.05% (m/v) NaOH
Flow rate of reducing agent	0.3 ml min^{-1}
Flow rate of sample	0.3 ml min^{-1}
Flow rate of carrier gas 1 (Ar)	0.9 l min^{-1}
Flow rate of carrier gas 2 (Ar)	0.2 l min^{-1}
Sample acidity HCl	3 N

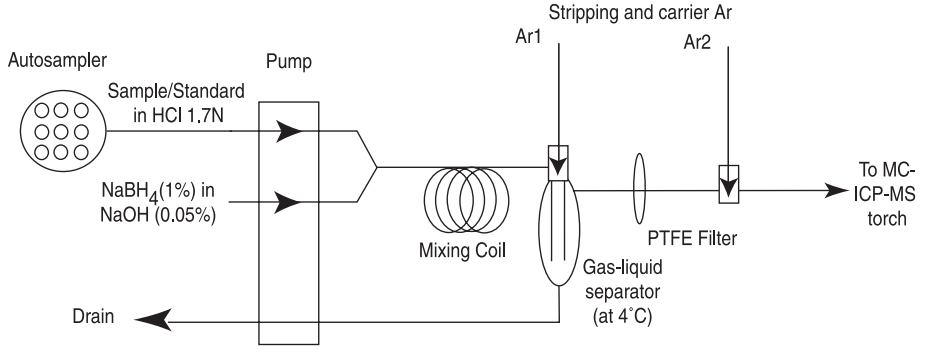

Fig. 1. Schematic diagram of the continuous-flow hydride generator (Rouxel et al., 2002).

ques (CRPG), has been used for the measurements of Sb isotopes. The instrumental settings are given in Table 1. This instrument consists of a standard ICP source and magnetic mass analyzer, which incorporates an RF-only hexapole collision cell technology (Turner et al., 1998). By addition of small amounts of gas to the collision cell, such as Ar, at few ml min^{-1} (typically 1.8 ml min^{-1}), the interactions of ions from the plasma with the collision gas reduce the energy spread of the ions from 20 to 30 eV to less than 1 eV.

The mass spectrometer is equipped with nine Faraday cups, and the collector setting is given in Table 2. Background correction (Z1−Z2) was made for each block of 25 data (10 s of counting time). The isotopic results are reported in the same manner as proposed for Fe, Cu and Se isotope measurements by MC-ICP-MS (Belshaw et al., 2000; Zhu et al., 2000; Rouxel et al., 2002). This method involves the measurement of an internal standard (Spex Sb elemental standard solution) between samples yielding the isotopic composition of the sample expressed as a deviation relative to the standard following the equation

$$\varepsilon^{123}\mathrm{Sb} = 10,000\left(\frac{R_{\mathrm{spl}}}{R_{\mathrm{std}}} - 1\right)$$

where R_{spl} is the measured $^{123}Sb/^{121}Sb$ ratio for the unknown sample and R_{std} is the mean $^{123}Sb/^{121}Sb$ ratio of the standard Spex hereafter referred to as "matching standard" (MS) measured before and after each sample. Each data point given in this study corresponds to the mean of three replicate measurements of individual bracketed samples. The MS and the sample are analyzed at the same concentration with less than 25% difference.

Because hexapole cell technology may produce complex polyatomic interferences, the background on Sb isotope was verified to be free of interferences by measuring blank solutions. Residual signal corresponds to Sb memory, mainly in the hydride generation system, and has an isotope ratio, within the uncertainty, similar to the standard isotope ratio. During each analytical session, and after passing a rinse solution of 3 N HCl for 5 min, the level of this memory is typically 1% of the previous Sb intensity measured and does not require any specific correction for most samples. Memory effects were, however, carefully monitored and washout time was extended to 10 min if required. Procedure blanks from all the analytical steps have been estimated at 0.3 ng.

Table 2
Collector setting

	Axial	High 1	High 2	High 3	High 4	High 5
Z1	120.4	121.4	122.4	123.4	124.4	125.4
Z2	119.6	120.6	121.6	122.6	123.6	124.6
1	^{120}Sn (+Te)	^{121}Sb	^{122}Sn (+Te)	^{123}Sb	^{124}Sn	(^{125}Te)

Because of the high H content of the gas introduced in the plasma torch, we verified that no interferences from SnH^+ on ^{121}Sb or SbH_2^+ on ^{123}Sb may bias the Sb isotopes analysis. For both elements, SnH and SbH have been found to be below 0.1% of the Sn and Sb signal. Furthermore, Sb is chemically separated from Sn using a cation exchange resin. Because element hydrides may form in the *Isoprobe* when using a mixture of Ar and H in the reaction collision cell (Rouxel et al., 2002), we used only Ar as collision gas. A spectral interference on ^{123}Sb isotope from ^{123}Te with isotopic abundance of 0.9% was found to be negligible in both standard solution and chemically purified samples, and no correction for Te interferences was required. Nonetheless, the intensity of ^{125}Te is monitored during each analysis. Sn is always present as impurity either in blank or sample solution and contributes at a typical level of 100 mV. This Sn pollution is probably derived from reagent used in the $NaBH_4$ solution but, as discussed in Section 4.1, this impurity does not produce any bias in the Sb isotope analysis.

3. Experimental results

3.1. Matrix effects and analytical accuracy

3.1.1. Internal accuracy

As the analytical precision of the "standard-sample bracketing" method depends on the stability of the instrumental mass bias, we measured the long-term evolution of the standard within an analytical session. The Sb isotope ratios measured are presented in Fig. 2, either as absolute notation or relative notation using ε units. The internal precision of the measurement corrected using the "standard-sample bracketing" is evaluated by the measurement of the matching stand-

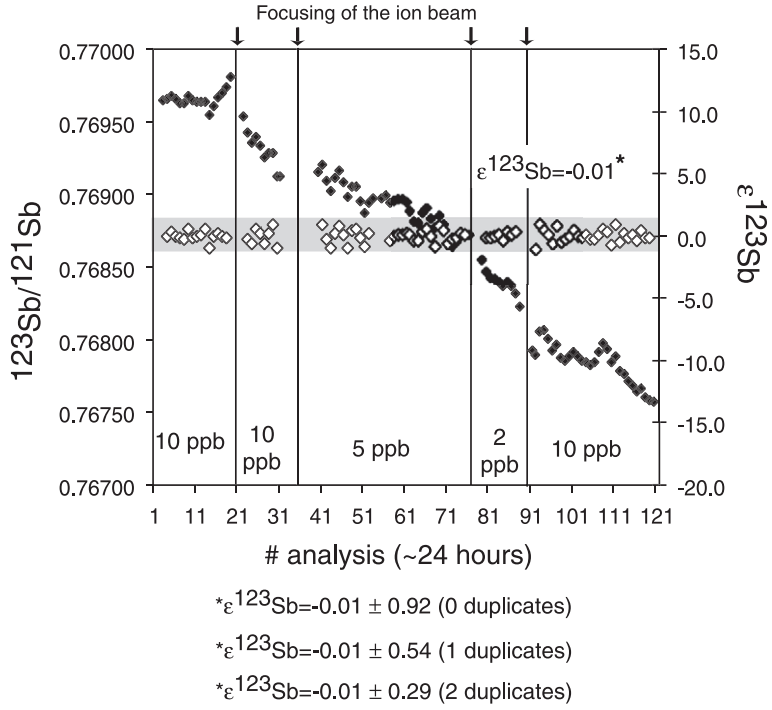

Fig. 2. $^{123}Sb/^{121}Sb$ ratio and corresponding relative $\varepsilon^{123}Sb$ notation for Sb internal standard (Spex solution) over a 24-h period. Filled diamonds correspond to uncorrected data whereas open diamonds correspond to sample-standard bracketed data. Duplicate bracketed measurements increase the internal precision and for three measurements, a precision of 0.20 ε units is obtained. During the analysis session of 24 h, the Sb concentration and the focus setting in solution were changed.

ard solution treated in the same way as for an unknown sample. The replicate measurements of the standard calculated in this manner are presented in Fig. 2. The precision for a single analysis of the standard is calculated at 0.92 ε units (95% confidence level) whereas for triplicate measurement as done for all samples, the precision is calculated at 0.29 ε units. The important implication of the analytical results is that, despite the long-term or more short-term variations of the instrumental mass bias (up to 25 ε units in 24 h), the internal precision reached is largely sufficient for sample analysis. As a direct observation from Fig. 2, the long-term evolution of the instrument is regular and decreases with time. This evolution is not influenced by the focus lens setting (Fig. 2) and is probably related to similar source effects, which have been observed in most MC-ICP-MS (Rehkämper et al., 2000). Another possibility is the aging of the $NaBH_4$ reagent, which may produce a change in the H_2 flow rate in the plasma torch and thus affect the Sb ionization conditions. However, it should be pointed out that no systematic trend of the instrumental mass bias can be defined and the bias is not reproducible between different analytical sessions. The second important observation is that the concentration of Sb analyzed (between 2 and 10 ppb) has no major effect on the precision or on the instrumental mass bias.

3.1.2. Matrix effects

In the course of the analytical development, it was observed that Sb was not reduced or only partially reduced to Sb(III) by the KI and ascorbic acid mixture when more than 5 mg of Fe(III) was present in solution. This is consistent with a previous study (Sanz et al., 1990) of the interference of Fe for the determination of Sb by hydride generation. The mechanism proposed to explain this interference is based on the fact that Fe(III) can oxidize Sb(III) to Sb(V). Taking into account that the normal reduction potential of the Sb(V)–Sb(III) system is 0.75 mV and

that of the Fe(III)–Fe(II) system is 0.77 mV, Sb(V) is not likely to be reduced until Fe(III) is present in solution. Therefore, chemical purification through cation-exchange resin is required to obtain quantitative and stable reduction of Sb(V) to Sb(III).

The effect on other hydride-forming elements in the determination of Sb by hydride generation has been studied previously (Hall and Pelchat, 1997) and this study suggests that no interferences (i.e. signal suppression) are expected for solutions with 1000-fold levels of As or Se. In this study, we also assessed the effect of Ge and Sn in addition to As and Se on Sb sensitivity and the instrumental mass bias effect. As evident from Table 3, Sb isotope composition of the standards does not deviate from the true values when doping the matrix with various proportion of other hydride-forming element.

After the chemical separation by cation-exchange resin, Sb isotope can be measured directly by HG-ICP-MS without further purification, as Fe(III) has been removed. However, to ensure that the analytical procedure can be applied for a large range of sample types (i.e. organic-rich material, sulfides, seawater), and other hydride-forming elements concentrations, we always purified Sb using thiol cotton fiber. It has been shown that cotton impregnated with thioglycollic acid, "thiol cotton fiber" (TCF), strongly adsorbs elements such as Se, Te, As and Sb depending on their various oxidation states (Yu et al., 1983). The major advantages of using this method for the determination of Sb isotopes by hydride generation MC-ICP-MS are: (1) the affinity of TCF for Sb(III) is very high, allowing the achievement of complete separation of Sb(III) species from Sb(V) species and also avoiding any possible mass fractionation during chemical separation; (2) removal of residual matrix interfering elements for hydride generation such as transitional metals; (3) quantitative separation of other hydride-forming elements such as Se, Ge, As and the isobaric interference of Te. After this final step, the solution of Sb(III) in 0.5% KI and 3 N HCl is stable over a 6-month period.

3.1.3. External reproducibility

Because Sb isotopes can be fractionated during acid leaching, reduction steps and chemical separation using TCF, we verified that the yield for Sb at each step of chemical purification was complete. In Table

Table 3
Standard reproducibility

	Purification step	Sb (ng)	Yield (%)	ε^{123}Sb
Sb Spex	(1)	50	102	0.36
Sb Spex	(1)+(2)	100	91	0.07
Sb Spex	(1)+(2)	100	84	−0.28
Sb Spex	(1)+(2)	50	94	−0.03
Sb Spex	(1)+(2)	50	98	0.05
Sb Spex	(1)+(2)+(3)	50	91	0.03
Sb Spex	(3)	100	99	−0.18
Sb Spex	(3)	100	96	0.18
Sb Spex	(3)	100	98	0.01
Sb Spex	(3)	50	96	−0.17
Sb Spex[a]	(3)	100	111	−0.11
Sb Spex[a]	(3)	100	99	−0.21
Sb Spex[a]	(3)	100	96	0.22
Sb Spex[a]	(3)	100	98	0.0
Sb Spex[a]	(3)	100	101	−0.41
Sb Spex	(3)	50	102	0.26
Average			97	−0.01
2 S.D.			12	0.40
Sb Spex[b]		10		−0.26
Sb Spex[b]		10		−0.15
Sb Spex[b]		10		−0.04
Sb Spex[b]		10		0.11
Sb Spex[b,c]		10		0.02
Sb Spex[b,d]		10		−0.07
Sb Spex[b,d]		10		0.09
Sb Spex[b,d]		10		0.11
Sb Spex[b,d]		10		0.33
Sb Spex[e]		10		0.11
Sb Spex[e]		10		0.11
Average			82	0.03
2 S.D.			78	0.32
Sb Spex[f]	(3)		29	−11.7
Sb Spex[f]	(3)		37	−6.9
Sb Spex[f]	(3)		38	−6.6
Sb Spex[f]	(3)		38	−5.8
Sb Spex[f]	(3)		38	−6.8
Sb Spex[f]	(3)		38	−5.7
Sb Spex[f]	(3)		39	−7.4
Sb Spex[f]	(3)		27	−11.6
Sb Spex[f]	(3)		56	−6.8
Sb Spex[f]	(3)		70	−4.5

S.D., standard deviation.
(1) Acid dissolution + evaporation; (2) purification through AG50-X8; (3) purification through TCF.
[a] Sb solution doped with Se, Ge, As, Te (Se/Sb = 1; Ge/Sb = 10; As/Sb = 50; Te/Sb = 1).
[b] Sb solution doped with Ge, As (Ge/Sb = 10; As/Sb = 10).
[c] Sb solution doped with As (As/Sb = 100).
[d] Sb solution doped with Sn (Sn/Sb = 100).
[e] Sb solution in 1.5 N HCl and matching standard in 3 N HCl.
[f] Sb solution doped with basalt matrix (250 mg).

3, Sb yield and isotope composition have been determined for standards doped between each step of the chemical separation. The results are, within uncertainty, undistinguishable from the true value and we assigned therefore a precision of 0.4 ε units (at 95% confidence level) for all data presented in this study. This external reproducibility is further verified by analyzing in replicate several georeference materials (Govindaraju, 1994), and the results are presented in Table 4.

3.2. Isotopic fractionation between Sb(III) and Sb(V) species

The isotopic fractionation factors between the coexisting Sb(III) and Sb(V) species have been investigated both during analysis and after chemical separation by TCF. For the reduction experiment of Sb(V), the reducing agent used was KI and ascorbic acid mixture, as classically used for Sb(V) reduction.

The hydride generation technique is considered to be selective relative to Sb(III) at pH between 2 and 8 (Dedina and Tsalev, 1995) and can therefore be used to separate and determine the isotopic composition of Sb(III) species in Sb(III) and Sb(V) mixtures. A solution of Sb(V) at 10 ppb was prepared by diluting in HCl a stock of Spex standard solution of 5 ppm in 0.05 N HNO_3. KI was added in an open vessel placed on a hot plate stirrer. KI and ascorbic acid concentration in the reaction vessel for all experiments was 0.05%. This solution was continuously analyzed by HG-MC-ICP-MS (on-line experiments) and the Sb isotope acquisition was made every 60 s. Instrumental mass bias was corrected by measuring the Sb(III) standard solution (Spex standard) stored in 0.5% KI and ascorbic acid medium at the beginning and the end of the experiment. Under the experimental conditions, Sb(V) reduction is complete in ~ 15 min and the estimated precision of ε^{123}Sb is ~ 1 ε unit.

Under the analytical condition of the experiments, 20–50% of Sb(V) formed volatile hydride. Therefore, the experimental data have been corrected for Sb(V) contribution of Sb(III) analysis. This correction assumes that a constant fraction of Sb(V) species forms volatile hydride through all the experiment

Table 4
Sb isotope composition of selected georeference materials and duplicated analysis

Sample	Description	Sb[a] (ppm)	ε^{123}Sb					
			#1	#2	#3	#4	Average	2 S.D.
Igneous rocks-basalt								
BHVO-1		0.16	1.7	1.3	1.7		1.5	0.4
BR		0.16	3.2	2.8	2.7	3.1	2.9	0.5
Other silicate rocks								
DR-N	Diorite	0.42	2.8	2.7	2.6		2.7	0.3
DTS-1	Dunite	0.50	0.2	0.4			0.3	0.3
GA	Granite	0.20	2.4	2.3			2.3	0.2
PCC-1	Peridotite	1.28	−0.6	−0.3			−0.5	0.4
WS-E	Dolerite	0.08	0.7	0.3			0.5	0.5
Environmental samples								
BCR-176	City Waste incineration Ash	413.7	0.3					
GSD-3	Stream sediment	5.4	1.9	1.5	1.7	1.6	1.7	0.3
GXR-1	Jasperoid	118	0.5					
GXR-4	Copper mill-head	4.80	4.9	4.8	4.6		4.8	0.3
GXR-5	Soil	1.63	1.3	1.6	1.4		1.4	0.3
GXR-6	Soil	3.60	2.4	2.6	2.8		2.6	0.3
SDO-1	Ohio shale	2.10	2.4	2.1	2.5		2.3	0.4

S.D., standard deviation.
[a] After Govindaraju (1994).

and that the reaction rate is first order with respect to Sb(III) concentration. The Sb isotope fractionation process is considered to follow a Rayleigh-type process. Modeled Sb yield and Sb isotope compositions are plotted in Fig. 3 together with experimental results. For two duplicate experiments, we obtained an instantaneous Sb isotope fractionation factor of 8.8 and 9.0 ε units for the reduction of Sb(V) to Sb(III) species. The agreement for modeled and measured Sb isotope composition, as presented in Fig. 4, suggests that experimental results are fully explained by a kinetic process. As these two replicate experiments were made under similar conditions, the possible effects of reducing agent and reduction reaction rate on Sb isotope fractionation have not been assessed.

The chemical separation of Sb species (i.e. off-line experiments) was performed using TCF as described below. As already observed by Yu et al. (1983), Sb(III) was selectively adsorbed on a TCF column in an acid medium with a HCl molarity below 0.01 N, whereas nonsorbed Sb(V) passes through the column. The Sb(V) reduction experiments were made in an H_2O medium for 1 h by adding various amounts of KI and ascorbic acid. The results obtained suggest that ε^{123}Sb values of Sb(III) and Sb(V) follow a kinetic (Rayleigh) model with an isotope fractionation factor of 5.5 ε units (Fig. 5). We are aware that some species transformation (i.e. Sb(V) reduction) may occur during column separation and that part of the isotope fractionation observed may be overprinted by the in situ isotope fractionation. However, under the same analytical conditions but without the KI and ascorbic acid reduction step, no Sb was found to be adsorbed onto TCF column, suggesting that in situ reduction of Sb(V) is not unlikely.

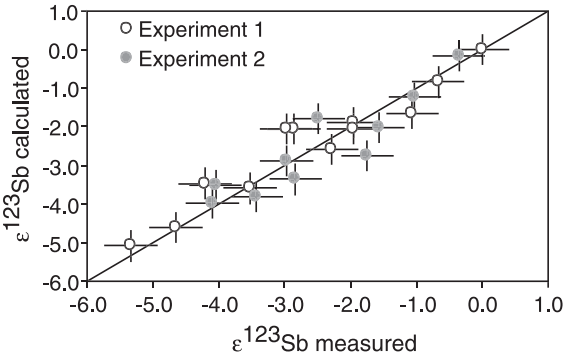

Fig. 4. Correlation following a 1:1 line between measured and modeled ε^{123}Sb presented in Fig. 3 for experiments 1 and 2.

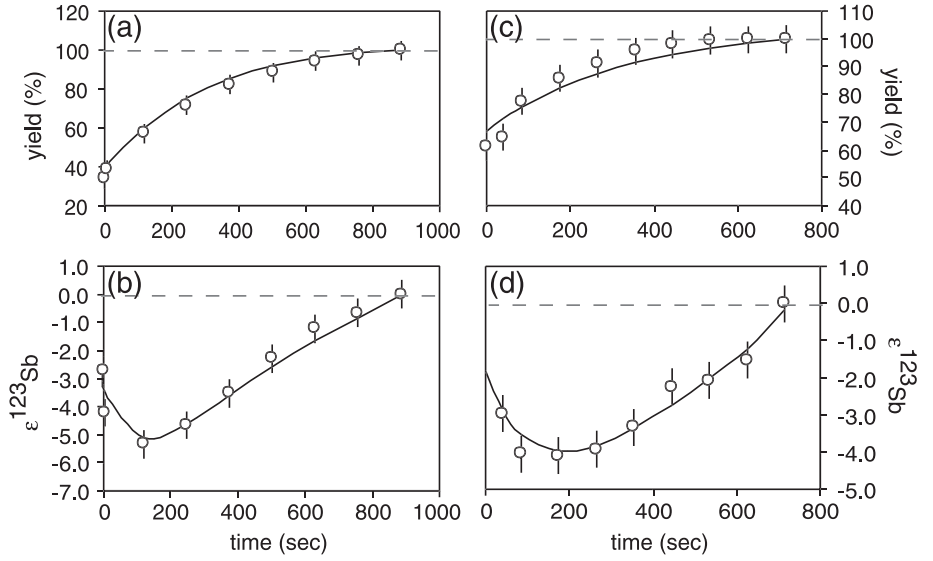

Fig. 3. Results of experimental investigation of Sb(V) reduction to Sb(III) using a mixture of KI and ascorbic acid (at 0.05%) in 0.4 N HCl medium for experiment 1 (plots a and b) and 1 N HCl medium for experiment 2 (plots c and d). Solid lines are modeled for the evolution of the Sb yield (corresponding to the percent of signal measured relative to maximum signal obtained after completed reduction) and ε^{123}Sb. See text for discussion.

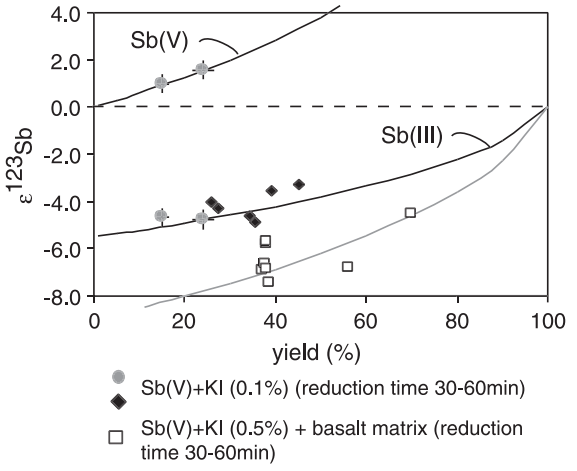

Fig. 5. Diagram showing ε^{123}Sb values for Sb(III) and Sb(V) species relative to the yield of Sb(III) reduction. Sb species have been separated using TCF as described in text. Two black lines represent the modeled evolution of ε^{123}Sb following a Rayleigh-type fractionation with a fractionation factor of 5.5 ε units, whereas the light gray line corresponds to Sb(III) kinetic fractionation with a 9 ε unit fractionation factor.

For standards doped with a basalt matrix, partial reduction of Sb(V) was obtained (Table 3) as discussed above, and the Sb isotope composition of Sb(III) species corresponds to the instantaneous isotope fractionation of about 9 ε units. This isotope fractionation factor is therefore 3.5 ε units greater than for matrix-free experiments, which suggest a different and more complex reduction process in the presence of other elements.

4. Results and discussions

4.1. Sb isotope composition of seawater

North Atlantic deep seawater (36°13.8′N, water depth of 2270 m) samples were taken using the IFREMER hydrocast unit (rosette fitted with 16 × 8 l bottles) during the IRIS cruise (chief scientist Y. Fouquet) in June 2001. Immediately upon recovery, for each sample, 40 ml of seawater were filtered through a 0.45-μm polypropylene filter, and passed through a TCF column to separate Sb(III) species from Sb(V) species. Reduction and separation of Sb(V) species were made 2 months later.

Coastal surface seawater samples were collected at the same site in west Brittany (France) and split to analyze separately total Sb in filtered and nonfiltered samples. Results are presented in Table 5 and Fig. 6. The concentration of Sb obtained is in accordance with measurements of Cutter and Cutter (1998), who obtained a Sb concentration of 161 ng/l ± 50 for North Atlantic Seawater. We found a Sb concentration in North Atlantic to be 166 ng/l ± 9 in both deep seawater and surface seawater. The pentavalent antimony is the predominant species in samples studied and despite the fact that Sb(III) recovered was too low to permit isotopic composition measurement, it is unlikely that the Sb isotope composition of Sb(III) will change the Sb isotope composition of total Sb in seawater. Our results suggest therefore that ε^{123}Sb value of seawater is homogeneous throughout the depth profile and probably for all locations in the North Atlantic. It has been suggested that the profile of dissolved Sb in seawater is that of a mildly

Table 5
Sb isotope composition of seawater

	Depth (m)	Sb(III) (ng/l)	Sb(V) (ng/l)	SbT (ng/l)	ε^{123}Sb
North Atlantic coastal seawater (France, Brittany)					
#1	0.3			161	3.9
#2	0.3			170	3.6
#3	0.3			167	3.7
#4	0.3			165	4.1
North Atlantic deep seawater[a]					
CTD3-16	1000	16	155	171	3.6
CTD3-16	1000	11	155	166	3.8
CTD3-15	1500	10	163	173	3.9
CTD1-14	1600	6	150	156	3.4
CTD3-14	1600	10	143	153	3.2
CTD1-12	1700	1	155	156	4.1
CTD1-10	1725	5	163	168	3.7
CTD1-8	1775	6	149	155	3.8
CTD1-6	1800	10	162	172	3.7
CTD5-6	1800	10	159	169	4.7
CTD1-4	1850	9	171	180	3.1
CTD1-2	1925	12	162	174	4.2
CTD5-1	2000	4	155	158	3.0
Mean		8	157	166	3.7
2 S.D.		4	7	9	0.4
Sb standard purified			100		0.1
Sb standard purified			103		−0.4
Blank			0.3		

S.D., standard deviation.
[a] ε^{123}Sb reported only for Sb(V) species.

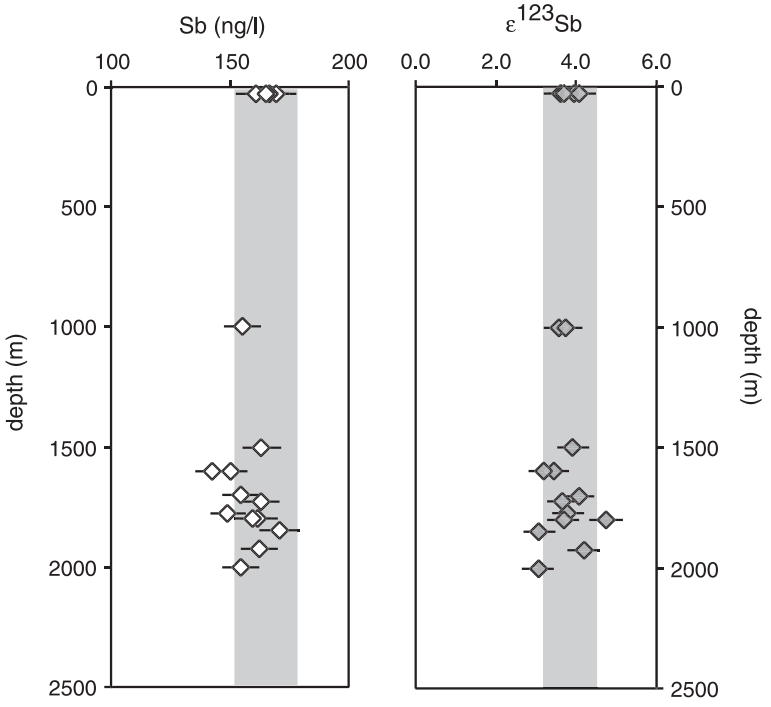

Fig. 6. Sb concentration and ε^{123}Sb values of seawater sampled in North Atlantic. The gray zone corresponds to the mean value and suggests that within analytical uncertainty, no variation in Sb concentration and Sb isotope composition is observed along the depth profile. Individual data are presented in Table 5.

scavenged element with surface (atmospheric) input, and is strongly influenced by the mixing of water masses with different Sb concentration (Cutter and Cutter, 1998) having been affected by loss due to scavenging during transport.

The Sb concentration and ε^{123}Sb values of seawater at 3.7 ± 0.4 obtained in this study (Fig. 6) suggest that that Sb is a "quasi conservative" element.

4.2. Isotopic composition of mantle-derived rocks and sediments

Preliminary results on Sb isotopic compositions of selected geological materials including basalts, soil and sediments (Tables 4 and 5) show a variation of 5.5 ε units, which is more that 10 times higher than the analytical precision. This demonstrates the existence of natural variations of the Sb isotopic composition, as suggested by experimental investigations during Sb(V) reduction.

For two igneous rocks, BR (continental basalt) and BHVO-1 (Hawaiian basalt), we obtained ε^{123}Sb values of 2.9 and 1.5, respectively. These results showing ε^{123}Sb variations of 1.5 ε units are surprising and may be related to heterogeneities in magma sources or to metasomatic fluid contamination as Sb is considered a fluid-mobile element (Noll et al., 1996). Further studies are, however, required to address this issue. Other silicate rocks (Table 4) display a larger range of 3 ε units, but the cause of the variability is presently unclear and post-depositional processes such as alteration may complicate the interpretations.

Environmental samples studied are enriched in Sb relative to crust values and most of them are associated with ore deposits or waste material and a variations of Sb isotope data of 4.5 ε units is observed. The processes of Sb remobilization and enrichment in these deposits should play an important role in Sb isotope fractionation.

For deep-sea sediments (Table 6), the obtained range of Sb-isotopic compositions is between 0.9

Table 6
Sb isotope composition of selected natural samples

Sample	mbsf[a]	Description	Sb (ppm)	ε^{123}Sb #1	ε^{123}Sb #2
Deep-sea sediments					
Site ODP 1149, Leg 185					
1149A-1H1,140	1.4	Ash- and silica-bearing clay	0.72	2.1	
1149A-4H2,140	26.1	Clay	0.87	2.2	
1149A-7H4,140	57.6	Ash-bearing siliceous silty clay	0.65	0.9	1.2[b]
1149A-10H3-140	84.6	Ash-bearing siliceous clay	1.21	2.0	1.6[b]
1149A-14H2-140	121.1	Pelagic clay	1.34	2.8	2.7[b]
1149A-18H3-140	160.4	Pelagic clay, faint fault trace	1.34	2.8	2.7[b]
1149A-20X1-140	171.2	Pilt-bearing clay	1.84	1.8	2.0[b]
Hydrothermal sulfides					
Menez Gwen					
DV-16-03a		Marcasite in low-*T* slab diffuse flow	22.1	16.9	
DV-16-03b		Ditto	22.6	15.2	15.8
Lucky Strike					
DV-6-2		Fresh volcanic glass from lava lake	0.12	2.4	
ALV-2606-3-2 py		Marcasite blades in chimney conduit	2.6	5.1	
DV-02-01 py		Porous chimney with bladed aggregates of marcasite	64.1	3.8	3.3
DV-18-5B2		Ba- and Zn-rich flange fragment	59.8	5.0	
FL-18 fond		Large granular aggregate of euhedral sphalerite	378.5	3.4	
FL-19-05 py		Porous zone of chimney composed of massive to fine grains pyrite with marcasite	3.1	4.0	3.6
FL-19-08a py		Massive pyrite and marcasite aggregate	20.0	3.7	
FL-19-08b py		Ditto	2.8	5.2	
FL-19-09a py		Coarse euhedral pyrite filling internal zone of chimney	17.3	5.1	
FL-19-09b py		Ditto	2.7	6.1	
FL-24-02 mar		Flange composed principally of massive marcasite and dendritic sphalerite in internal zone, matrix of barite	71.7	4.6	
FL-24-02 sph		Ditto	161.6	2.3	3.0
FL-24-02b mar		Ditto	52.1	3.8	
FL-24-04 py		Fine euhedral aggregates of marcasite lining large tortuous conduit	2.1	2.4	
Lau Basin					
NL-07-06-2 bulk		White Church site	323.4	2.6	
NL-10-04 sph		White Church site	225.8	2.6	
NL-16-02 py		Hine Hina site	187.7	− 2.2	

[a] Meters below seafloor.
[b] ε^{123}Sb values measured after passage through cation-exchange resin.

and 2.8 ε units with a mean of 2 ε units, which is significantly lower than seawater Sb and closer to the range of continental silicate rocks as can be seen from the summary of data in Fig. 7.

Despite the limited amount of samples studied, we define a preliminary bulk oceanic and continental crust at 2.0 ε units, based on the ε^{123}Sb values of mantle-derived rocks and deep-sea sediments. The apparent difference between the seawater composition and this value requires a study of Sb sources and sinks in oceanic system. Sb is known to be strongly associated with hydrous oxides of Mn and Fe in sediments (Brannon and Patrick, 1985). In particular, Sb is associated with the Mn-oxide fraction of deep-

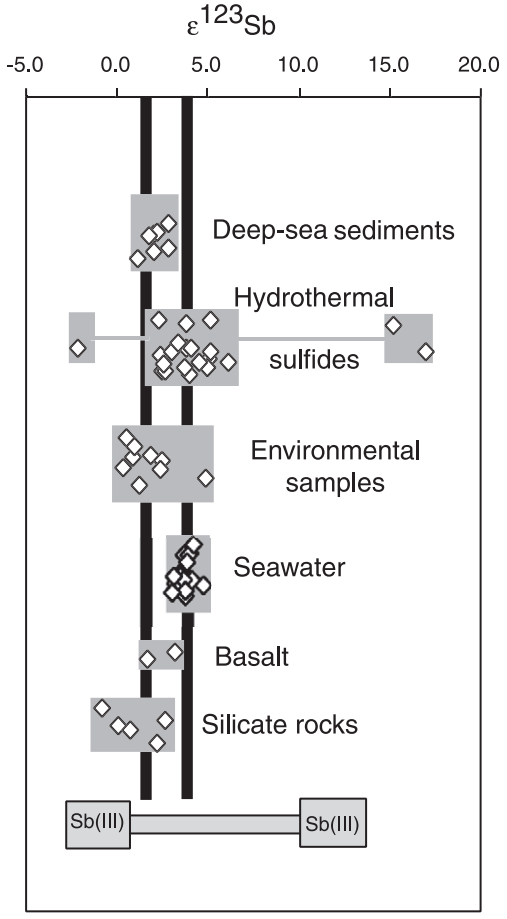

Fig. 7. Summary of Sb isotope compositions reported in this study for natural samples, such as mantle-derived rocks, deep-sea sediments, environmental samples, seawater and seafloor hydrothermal sulfides. Kinetic Sb isotope fractionation range for the reduction of Sb(V) to Sb(III) is also illustrated for comparison.

sea sediment and it may be strongly enriched in ferromanganese nodules relative to pelagic clays (Li, 1982). Under anoxic conditions, Sb(III) species predominate (Andreae and Froelich, 1984) and may become actively scavenged onto particles or may accumulate in oxic or weakly reducing boundary in deep-sea sediments (Thomson et al., 1993). Following the approach of Barling et al. (2001) for Mo-isotope systematics, it can be anticipated that a study of anoxic and oxic sediments should clarify if the anoxic sink, dominated by Sb(III) species, and the oxic sink, dominated by Sb(V) species, are characterized by specific Sb isotope signatures.

4.3. Sb isotope in seafloor hydrothermal systems

The understanding of the behavior of Sb in geothermal systems and its transport in hydrothermal solutions has been the subject of numerous studies on the nature of antimony complexes in aqueous solutions (Krupp, 1988; Wood, 1989; Spycher and Reed, 1989; Oelkers et al., 1998; Tossell, 1994; Vink, 1996; Sherman et al., 2000). It is generally assumed that only Sb(III) sulfide complexes are important for antimony transport under hydrothermal conditions. However, Sb(V) sulfide complexes may be stable in alkaline solutions under the reducing conditions of hydrothermal ore deposits (Sherman et al., 2000), but this hypothesis is not relevant for most seafloor hydrothermal systems. Moreover, these experimental studies suggest that Sb oxidation or reduction processes may be ubiquitous in hydrothermal systems and we postulate that Sb stable isotope ratios could be used as indicators of hydrothermal processes, providing further constraints on the redox conditions of the systems and the sources of metals deposits.

We analyzed a set of hydrothermal deposits, which included pyrite-, marcasite- and sphalerite-rich deposits from various hydrothermal fields. These include the Menez Gwen and Lucky Strike hydrothermal fields (Fouquet et al., submitted for publication) located on Mid-Atlantic Ridge, as well as the Lau Basin field located in back-arc systems (Fouquet et al., 1991). Sb concentration, sample description and Sb isotope composition are presented in Table 6 and the range of ε^{123}Sb values obtained are compared with other sample types in Fig. 7. These data show a large spread of ε^{123}Sb values up to 18 ε units. As pointed out in Fig. 7, only two samples are clearly outside the range defined by seawater (3.7 ε units) and basalts at Lucky Strike (defined at 2.2 ε units). Another interesting observation is that all the data except one sample at Lau Basin, Site Hine Hina, have ε^{123}Sb values systematically higher than basaltic values.

The behavior of Sb and other trace metals in seafloor sulfide deposits has been reviewed by Hannington et al. (1991). Despite a wide range of concentrations in most sulfide deposits with similar source rocks, Cu-rich and Zn-rich assemblages display consistent enrichments and depletions of trace elements. In this context, Sb is found to be enriched in Zn-rich deposits and correlates with Pb, Cd and Ag.

Sb concentration has also been determined in some vent fluids from various locations (Douville et al., 1999) and the data suggest that Sb is also preferentially enriched in back-arc basin hydrothermal systems relative to mid-ocean ridge hydrothermal systems. An important aspect of Sb geochemistry in hydrothermal fluids is that Sb may be enriched or depleted relative to seawater. This suggests that Sb derived from seawater may be effectively incorporated in seafloor hydrothermal systems, reduced subsequently to Sb(III), and then precipitated as sulfides in chimney environment. In the light of our results on Sb isotope fractionation during Sb reduction, we consider seawater Sb(V) reduction in hydrothermal systems to be the most likely process to account for our present data. Therefore, considering that seafloor hydrothermal systems are dynamic systems whereby seawater penetrates at different levels between the reaction and the discharge zones (Alt, 1996), it is expected that the Sb(V) remaining in solution becomes progressively enriched in the heavier isotope along its flow path. As seawater interacts with the substratum or the hydrothermal fluid, Sb(III) is progressively lost, either as sulfides or adsorbed onto metal hydroxides. The sulfides sampled at Menez Gwen are located within hydrothermal slabs where low-temperature diffuse venting occurs (Fouquet et al., submitted for publication) and are highly fractionated up to 10 ε units relative to seawater. Sb concentration in hydrothermal fluid at Menez Gwen has been determined at <3 nM (Douville et al., 1999), which is less than a two-fold enrichment of Sb relative to seawater. Considering an instantaneous Sb isotope fractionation of 9 ε units during reduction of Sb(V) to Sb(III), ε^{123}Sb values of 15 ε units would be easily reached by a fluid incorporating seawater depleted in 85% of the initial Sb(V).

During the alteration of the oceanic crust, antimony seems to display a dual behavior, being leached at high temperature at mid-ocean ridges (VonDamm, 1995) and being enriched by low-temperature seawater/basalt interaction at a ridge flank with enrichment factor in altered glass MORB up to 2000 (Jochum and Vema, 1995). Thus, our preliminary data on Sb isotope composition of hydrothermal sulfides suggest that Sb isotope systematics should provide extremely useful tracers for the study of seawater–rock interactions.

5. Conclusion

In this study, we have presented a method for a sensitive and precise determination of Sb isotopes by MC-ICP-MS using an on-line hydride generation system for sample introduction. Instrumental mass bias is easily corrected using the "standard-sample bracketing" method. An important advantage of this technique is the high sensitivity, which makes it possible to analyze Sb isotopes in 5 ng sample. The external precision is 0.4 ε units at 95% confidence level and allows identification of natural variations of Sb isotopes. Although the hydride generation system is by itself a method to isolate Sb from the geological matrix, a preconcentration step is required for accurate analysis. The preconcentration step removes not only the metals that suppress Sb hydride generation, but also Te, which causes isobaric interference. This method allows one to separate Sb(III) and Sb(V) species for isotope analysis and provides new opportunities for studying Sb geochemistry in redox environments in aquatic systems.

The Sb isotope fractionation experiment reported here indicates strong fractionation during Sb(V) reduction to Sb(III). Seawater, mantle-derived rocks, various environmental samples, deep-sea sediments and hydrothermal sulfides from deep-sea vents have been analyzed for their Sb isotopic composition, permitting the definition of a preliminary continental and oceanic crust reservoir at 2 ± 1 ε units. Seawater ε^{123}Sb values do not vary with depth and yield a value of 3.7 ± 0.4 ε units. Sb deposited in hydrothermal environments shows a significant range of Sb isotopic compositions (up to 18 ε units). These variations may reflect not only contribution from different Sb sources (such as seawater and volcanic rocks) but also kinetic fractionation occurring at low temperature in aqueous media through the reduction of seawater-derived Sb(V) in more reducing environment. On the whole, these preliminary results indicate high potential of Sb isotopes as paleoredox tracers in oceanic systems.

A further possible approach for Sb isotopes concerns the nature of Sb–microorganism interactions. Antimony oxidizing bacteria have been observed in the oxidizing zone overlying antimony ore deposits (Lyalikova, 1978) as well as in certain plant species that are antimony accumulators (Baroni et al., 2000). Experimental studies have evaluated the capacity of

microorganisms to selectively bioaccumulate antimony species (Pérez-Corona et al., 1997) and it has been suggested that the accumulated Sb(III) species do not seem to undergo any transformation in the uptake process. The possible identification of biologically induced Sb isotope fractionation is thus another important aspect for development of the study of Sb isotope systematics.

Acknowledgements

This work benefited from many fruitful discussions with Luc Marin. Technical support was provided by the PRISMS-EC grants, EC contract SMT4CT 98-2220 and financial support was provided by CNRS-INSU and IFREMER, contract 00/410.485. We thank Eric Oelkers, Xiangkun Zhu and Philippe Telouk for constructive reviews. **[EO]**

References

Alt, J.C., 1996. Hydrothermal alteration of the oceanic crust: mineralogy, geochemistry, and processes. In: Barrie, T., Hannington, M. (Eds.), Reviews in Economic Geology: Volcanic-Associated Massive Sulfide Deposits, vol 8. Soc. Econ. Geol., Chelsea, MI, pp. 133–155.

Anders, E., Grevesse, N., 1989. Abundances of the elements: meteoritic and solar. Geochim. Cosmochim. Acta 53, 197–214.

Andreae, M.O., 1983. The determination of the chemical species of some of the "hydride elements" (arsenic, antimony, tin and germanium) in seawater: methodology and results. In: Wong, C.S., Boyle, E., Bruland, K.W., Burton, J.D., Goldberg, E.D. (Eds.), Trace Metals in Sea Water. Plenum, New York.

Andreae, M.O., Froelich, P.N., 1984. Arsenic, antimony, and germanium biogeochemistry in the Baltic Sea. Tellus 36B, 101–117.

Andreae, M.O., Asmodé, J.-F., Foster, P., Van'tdack, L., 1981. Determination of antimony(III), antimony(V), and methylantimony species in natural waters by atomic absorption spectrometry with hydride generation. Anal. Chem. 53, 1766–1771.

Barling, J., Arnold, G.L., Anbar, A.D., 2001. Natural mass-dependent variations in the isotopic composition of molybdenum. Earth Planet. Sci. Lett. 193, 447–457.

Baroni, F., Boscagli, A., Protano, G., Riccobono, F., 2000. Antimony accumulation in *Achillea ageratum*, *Plantago lanceolata* and *Silene vulgaris* growing in an old Sb-mining area. Environ. Pollut. 109, 347–352.

Belshaw, N.S., Zhu, X.K., Guo, Y., O'Nions, R.K., 2000. High precision measurement of iron isotopes by plasma source mass spectrometry. Int. J. Mass Spectrom. Ion Process. 197, 191–195.

Belzile, N., Chen, Y.-W., Wang, Z., 2001. Oxidation of antimony (III) by amorphous iron and manganese oxyhydroxides. Chem. Geol. 174, 379–387.

Brannon, J.M., Patrick, W.H., 1985. Fixation and mobilization of antimony in sediments. Environ. Pollut. 9, 107–126.

Cutter, G.A., Cutter, L.S., 1998. Metalloids in the high latitude North Atlantic Ocean: sources and internal cycling. Mar. Chem. 61, 25–36.

Dedina, J., Tsalev, D.L., 1995. Hydride Generation Atomic Absorption Spectrometry. Wiley, Chichester, NY, 526 pp.

Douville, E., Charlou, J.-L., Donval, J.-P., Hureau, D., Appriou, P., 1999. As and Sb behaviour in fluids from various deep-sea hydrothermal systems. C.R. Acad. Sci., Earth Planet. Sci. 328, 97–104.

Ellis, A.S., Johnson, T.M., Bullen, T.D., 2002. Chromium isotopes and the fate of hexavalent chromium in the environment. Science 295, 2060–2062.

Fouquet, Y., Von Stackelberg, U., Charlou, J.-L., Donval, J.-P., Erzinger, J., Foucher, J.P., Herzig, P., Mühe, R., Soakai, S., Wiedicke, M., Whitechurch, H., 1991. Hydrothermal activity and metallogenesis in the Lau back-arc basin. Nature 349, 778–781.

Fouquet, Y., Charlou, J.-L., Donval, J.-P., Radford-Knoery, J., Ondreas, H., Costa, I., Lourenco, N., Segonzac, M., Tivey, M.K., Barriga, F., Cambon, P., Bougault, H., Etoubleau, J., 2003. Hydrothermal and volcanic processes on shallow hydrothermal fields near the Azores Triple Junction (Lucky Strike and Menez Gwen). Mar. Geol. (submitted for publication).

Govindaraju, K., 1994. 1994 Compilation of working values and sample description for 383 geostandards. Geostand. Newsl. 18, 1–158.

Gurnani, N., Sharma, A., Talukder, G., 1994. Effects of antimony on cellular systems in animals—a review. Nucleus 37, 71–96.

Hall, G.A.M., Pelchat, J.-C., 1997. Analysis of geological materials for bismuth, antimony, selenium and tellurium by continuous flow hydride generation inductively coupled plasma mass spectrometry: Part 1. Mutual hydride interferences. J. Anal. At. Spectrom. 12, 97–102.

Hannington, M., Herzig, P., Scott, S., Thompson, G., Rona, P., 1991. Comparative mineralogy and geochemistry of gold-bearing sulfide deposits on the mid-ocean ridges. Mar. Geol. 101, 217–248.

Jochum, K.P., Hofmann, A.W., 1997. Constraints on earth evolution from antimony in mantle-derived rocks. Chem. Geol. 139, 39–49.

Jochum, K.P., Vema, S.P., 1995. Extreme enrichment of Sb, Tl and other trace elements in altered MORB. Chem. Geol. 130, 289–299.

Johnson, T.M., Herbel, M.J., Bullen, T.D., Zawislanski, P.T., 1999. Selenium isotope ratios as indicators of selenium sources and oxyanion reduction. Geochim. Cosmochim. Acta 63, 2775–2783.

Krupp, R.E., 1988. Solubility of stibnite in hydrogen sulfide solutions, speciation and equilibrium constants, from 25 to 350 °C. Geochim. Cosmochim. Acta 52, 3005–3015.

Li, Y.H., 1982. Interelement relationship in abyssal Pacific ferromanganese nodules and associated pelagic sediments. Geochim. Cosmochim. Acta 46, 1053–1060.

Lyalikova, M.N., 1978. Antimony-oxidizing bacteria and their geochemical activity. In: Krumbein, W.E. (Ed.), Environmental Biogeochemistry and Geomicrobiology. Ann Arbor Science, Ann Arbor, pp. 929–936.

Maréchal, C.D., Télouk, P., Albarède, F., 1999. Precise analysis of copper and zinc isotopic compositions by plasma-source mass spectrometry. Chem. Geol. 156, 251–273.

Maréchal, C.N., Nicolas, E., Douchet, C., Albarède, F., 2000. Abundance of zinc isotopes as a marine biogeochemical tracer. Geochem. Geophys., 1.

Marin, L., Lhomme, J., Carignan, J., 2001. Determination of selenium concentration in sixty five reference materials for geochemical analysis by GFAAS after separation with thiol cotton. Geostand. Newsl. 25, 317–324.

Matthews, A., Zhu, X.K., O'Nions, K., 2001. Kinetic iron stable isotope fractionation between iron (-II) and (-III) complexes in solution. Earth Planet. Sci. Lett. 192, 81–92.

Noll, P.D., Newsom, H.E., Leeman, W.P., Ryan, J.G., 1996. The role of hydrothermal fluids in the production of subduction zone magmas: evidence from siderophile and chalcophile trace elements and boron. Geochim. Cosmochim. Acta 60, 587–611.

Oelkers, E.H., Sherman, D.M., Ragnarsdottir, K.V., Collins, C., 1998. An EXAFS spectroscopic study of aqueous antimony(III)-chloride complexation at temperature from 25 to 250 °C. Chem. Geol. 151, 21–27.

Pérez-Corona, T., Madrid, Y., Camara, C., 1997. Evaluation of selective uptake of selenium (Se(IV) and Se(VI)) and antimony (Sb(III) and Sb(V)) species by baker's yeast cells (*Saccharomyyces cerevisiae*). Anal. Chim. Acta 345, 249–255.

Petrick, K., Krivan, V., 1987. Radiotracer investigation of the interference of hydrofluoric acid in the determination of arsenic and antimony by hydride generation atomic absorption spectrometry. Anal. Chem. 59, 2476–2479.

Rehkämper, M., Halliday, A.N., 1999. The precise measurement of Tl isotopic compositions by MC-ICPMS: application to the analysis of geological materials and meteorites. Geochim. Cosmochim. Acta 63, 935–944.

Rehkämper, M., Schönbächler, M., Stirling, C.H., 2000. Multiple collector ICP-MS: introduction to instrumentation. Measurement techniques and analytical capabilities. Geostand. Newsl. 25, 23–40.

Rouxel, O., Ludden, J., Carignan, J., Marin, L., Fouquet, Y., 2002. Natural variations of Se isotopic composition determined by hydride generation multiple collector coupled mass spectrometer. Geochim. Cosmochim. Acta 66, 3191–3199.

Sanz, J., Martinez, M.T., Galban, J., Castillo, J.R., 1990. Study of the interference of iron and mercury in the determination of antimony by hydride generation atomic absorption spectrometry: use of speciation models. J. Anal. At. Spectrom. 5, 651–655.

Sherman, D.M., Ragnarsdottir, K.V., Oelkers, E.H., 2000. Antimony transport in hydrothermal solutions: an EXAFS study of antimony(V) complexation in alkaline sulfide and sulfide-chloride brines at temperatures from 25 °C to 300 °C at Psat. Chem. Geol. 167, 161–167.

Sims, K.W.W., Newsom, H.E., Gladney, E.S., 1990. Chemical fractionation during formation of the earth's core and continental crust: clues from As, Sb, W and Mo. Origin of the Earth. Oxford University Press, pp. 291–327.

Spycher, N.F., Reed, M.H., 1989. As(III) and Sb(III) sulfide complexes: an evaluation of stoichiometry and stability from existing experimental data. Geochim. Cosmochim. Acta 53, 2185–2194.

Thanabalasingam, P., Pickerign, W.F., 1990. Specific sorption of antimony(III) by the hydrous oxides of Mn, Fe, and Al. Water Air Soil Pollut. 49, 175–185.

Thomson, J., Higgs, N.C., Croudace, I.W., Colley, S., Hydes, D.J., 1993. Redox zonation of elements at an oxic/post-oxic boundary in deep-sea sediments. Geochim. Cosmochim. Acta 57, 579–595.

Tossell, J.A., 1994. The speciation of antimony in sulfidic solutions: a theoretical study. Geochim. Cosmochim. Acta 58, 5093–5104.

Turner, D.R., Whitfield, M., Dickson, A.G., 1981. The equilibrium speciation of dissolved components in freshwater and seawater at 25 °C and 1 atmosphere pressure. Geochim. Cosmochim. Acta 45, 855–881.

Turner, P.J., Mills, D.J., Schröder, E., Lapitajas, G., Jung, G., Iacone, L.A., Haydar, D.A., Montaser, A., 1998. Instrumentation for low- and high-resolution ICP-MS. In: Montaser, A. (Ed.), Inductively Coupled Plasma Mass Spectrometry. Wiley-VCH, New York, pp. 421–501.

Vink, B.W., 1996. Stability relations of antimony and arsenic compounds in the light of revised and extended Eh–pH diagrams. Chem. Geol. 130, 21–30.

VonDamm, K.L., 1995. Controls on the chemistry and temporal variability of seafloor hydrothermal fluids. In: Humphris, S.E., Zierenberg, R.A., Mullineaux, L.S., Thomson, R.E. (Eds.), Seafloor Hydrothermal Systems: Physical, Chemical, Biological, and Geological Interactions. American Geophysical Union, pp. 222–247.

Wood, S.A., 1989. Raman spectroscopic determination of the speciation of ore metals in hydrothermal solutions: I. Speciation of antimony in alkaline sulfide solutions at 25 °C. Geochim. Cosmochim. Acta 53, 237–244.

Yu, M.-Q., Liu, G.-Q., Jin, Q., 1983. Determination of trace arsenic, antimony, selenium and tellurium in various oxidation states in water by hydride generation and atomic-absorption spectrophotometry after enrichment and separation with thiol cotton. Talanta 30, 265–270.

Zhu, X.K., O'Nions, R.K., Guo, Y., Belshaw, N.S., Rickard, D., 2000. Determination of natural Cu-isotope variation by plasma-source mass spectrometry: implications for use as geochemical tracers. Chem. Geol. 163, 139–149.

Zhu, X.K., Guo, Y., Williams, R.J.P., O'Nions, R.K., Matthewsa, A., Belshaw, N.S., Canters, G.W., de Waal, E.C., Weser, U., Burgess, B.K., Salvato, B., 2002. Mass fractionation processes of transition metal isotopes. Earth Planet. Sci. Lett. 200, 47–62.